

E-CLOUD DEPENDENCE ON THE LONGITUDINAL BUNCH PROFILE IN THE PS AND THE HL-LHC

C. M. Bhat

Fermi National Accelerator Laboratory, Batavia, IL, 60510, USA,

H. Damerau, S. Hancock, E. Mahner, F. Caspers, G. Iadarola, T. Argyropoulos and
F. Zimmermann,
CERN, Geneva, Switzerland,

During the HL-LHC era [1] the bunch intensities in the LHC will go up by nearly a factor of two compared to the LHC-design values [2]. However, recent studies have shown that the prospects for significantly increasing bunch intensities in the LHC may be severely limited by the electron-cloud (EC) driven beam instability and the available cryogenic cooling capacity. This motivates exploration of additional EC mitigation techniques that can be adopted along with those already in place. Preliminary simulations indicated that “flat” bunches can be beneficial over Gaussian bunches to reduce the EC build up. Rigorous studies on realistic bunch profiles have never been carried out. Therefore, we have undertaken an in-depth investigation in the CERN PS via EC-simulations and beam experiments to see if we can validate the previous findings and, in particular, if flattening the bunch can be used as a potential EC mitigation technique. Finally, we perform an extrapolation to the HL-LHC scenarios.

PACS Codes: 29.20.-c, 29.27.Bd, 79.20.Hx

I. INTRODUCTION

After the first identification of an EC induced beam instability in 1965 and its cure by implementing a transverse feedback system in a small proton storage ring of the INP Novosibirsk by Budker and co-workers [3], significant research has been carried out at various accelerator facilities around the world [4-8] to understand the EC dynamics and on the possible mitigation techniques. Addressing the EC related issues has become one of the important topics for designing new circular high intensity lepton and hadron accelerators and, for upgrading the beam intensities in the existing accelerators.

The primary source of EC in these accelerators are interactions of the circulating charged particle beam with residual gas (i.e., by gas ionization) and/or by interactions of synchrotron radiation emitted by the circulating beam with the walls of the accelerator beam pipe. The former mechanism is relevant in medium energy hadron accelerators like CERN PS, SPS, Fermilab Booster and Main Injector etc. On the other hand, the latter mechanism plays a major role in many lepton accelerators and high energy hadron accelerators like the Large Hadron Collider (LHC) at CERN [2].

The LHC came into operation mid 2008. Over the past two years tremendous progress has been made from the point of view of its performance. The design goal of the LHC luminosity was $1 \times 10^{34} \text{ cm}^2 \text{ sec}^{-1}$ (with 25-ns bunch spacing) at a collision center of mass energy of 14 TeV. Currently, the LHC has reached more than 75% of its design peak luminosity at 57% of its design energy. For the High Luminosity LHC (HL-LHC) [1] two

bunch spacing scenarios – 25 ns and 50 ns – are under consideration. After the completion of the upgrade the peak luminosity (referred to as “peak virtual luminosity”) is expected to be in excess of $20 \times 10^{34} \text{ cm}^2 \text{ s}^{-1}$ and the bunch intensity to be increased by up to a factor of two with bunch brightness increased by a factor >4 .

At present, the LHC operates with a maximum of 1380 bunches with a bunch spacing of 50 ns and intensities of about 1.5×10^{11} ppb. The experiments carried out in 2011-12 showed that EC-driven vacuum problem in the LHC [9] was one of the major limiting factors for using 25-ns bunch spacing filling pattern in the present operation. This is the case despite several EC mitigation measures which had been adopted in the LHC, like saw-tooth pattern on the beam screen inside the cold dipole region, low secondary emission yield (SEY) NEG coatings on the inside surface of the warm beam pipes, etc. As a result, a major machine development campaign has been undertaken since 2011 to mitigate EC formation by beam scrubbing [10]. Consequently, significant improvement was seen [11] in the LHC performance. During the HL-LHC era the increased bunch intensity and the reduced bunch spacing will certainly aggravate EC related problems. Therefore, it is prudent to search for novel methods which could be complementary to beam scrubbing and can be used in combination with those already in places to reduce EC formation and, at the same time not detrimental to other proposed upgrade tasks at the LHC not related to the EC issues.

High-intensity bunches in the HL-LHC also face an additional issue related to single and multi-bunch instabilities driven by the loss of the Landau damping [12]. Research carried out in the CERN SPS using its 4th harmonic rf system [13] showed that the so-called bunch shortening mode renders the high-intensity beam more stable. Consequently, adding an 800 MHz Landau cavity is foreseen to stabilize high intensity beam in the LHC during the HL-LHC era [14]. The bunch-shortening mode increases peak line charge density of bunches, which may not be favourable with regard to EC. Therefore, it is quite important and pertinent to examine the implications of using a higher harmonic rf system in the HL-LHC from the EC point of view.

Preliminary simulation studies in the LHC indicated that there is an anti-correlation between increased bunch length and the electron cloud formation; long bunches with rectangular profile can reduce EC considerably [15]. But such bunches are presently not being considered for any of the LHC upgrade scenarios. On the other hand, an in-depth analysis using realistic but slightly flattened short bunches suitable for the LHC was never done. To shed light on this question, a dedicated EC experiment has been carried out in the CERN PS at ejection momentum of 26 GeV/c, where we investigated EC dependence on the shape of the bunch profiles. Fitting the EC simulations to the measurement data, we tried to study the correlation between bunch length and the EC evolution. Finally, we extrapolated our results to the HL-LHC scenarios by simulations studies.

Since 2007, the CERN PS has been equipped with a purpose-designed, dedicated one-meter long EC monitor in the straight section (SS) 98 [16]. It has two similar button pickups (BPU1 and BPU2) each shielded differently, and a stripline-type electrode. All three detectors and a vacuum gauge, situated near to BPU1, have been used to collect EC

signals and to monitor the correlated vacuum degradation, respectively. During the 2007 experiment with an average intensity of 1.15×10^{11} ppb, the EC build up has been observed on the LHC25 cycle (a train of 72-bunches with 25 ns bunch spacing) mainly for the last 36 ms before the beam ejection from the PS (*i.e.*, near “3rd Bunch Splitting” in Fig. 1(b)). Figure 1(a) illustrates a typical measured cumulative electrons from each pickup together with the vacuum pressure readings. An example of PS water-fall plot data [17] during the last 140 ms on the flat-top of the LHC25 cycle is shown in Fig. 1(b). During this time the beam undergoes quadrupole-splitting of 18 bunches similar to the one shown in Fig. 1(b) to finally produce a train of 72 bunches with 25 ns bunch spacing. Figure 1(c) shows the stages for rf turn-on sequences on the cycle. An approximate transfer function between the measured detector voltage signals (U_{BPU1}) and the electron line density (λ) has also been deduced using system impedance, button transparencies etc, which is given by, $\lambda/(e^-/\text{m}) = 2.3 \times 10^8 (U_{\text{BPU1}}/\text{mV})$ [16].

On the flat-top of the LHC25 cycle the bunch profile takes a variety of shapes and spans a range of bunch lengths. For example, during the 3rd bunch splitting dramatic bunch profile variation takes place in the double harmonic rf bucket made up of $h=42$ and $h=84$ rf systems (see for example Fig. 1(b)). Out at about 40 ms before the ejection, the 1σ bunch length is >4 ns as is shown in Fig. 2 (simulated using ESME [18]). Eventually, an adiabatic bunch compression followed by a rapid bunch rotation (which is a quasi-nonadiabatic process) in a combined $h=84$ and $h=168$ rf bucket shortens the bunches to the final 1σ -length of ≈ 0.75 ns at extraction. Phase space reconstruction of a single PS bunch at extraction using ESME and its comparison with the measured bunch profile is shown in the inset of Fig. 2. A very large growth in EC build up in correlation with the rapid decrease in the bunch length has been observed at the end of quarter bunch rotation (see Fig. 1(a)).

The current PS experiments have been performed with an emphasis on the EC measurements on bunch lengthening mode (BLM) and bunch shortening mode (BSM) in a controlled environment with adiabatically changing bunch shapes, exploiting the flexibilities of the PS rf system. The rf manipulations in this experiment was quite different from that used previously [16].

This paper is organized in the following way. We first give a brief review on the EC simulation model used in the present analyses. In Sec. III, we discuss the dedicated EC experiment in the PS and the data analysis. Sec. IV describes the EC simulations for the HL-LHC beam parameters. In the final section we summarize our findings.

II. E-CLOUD SIMULATIONS

The EC simulations have been carried out using E-CLOUD [19] and a newly developed code PyE-CLOUD [20]. Both E-CLOUD and PyE-CLOUD employ the same EC model, but the latter code uses new optimized algorithms with significant improvements in accuracy and speed. Both of these codes simulate EC cloud build up for the case when a train of bunches is injected into an empty accelerator section. The model assumes that

the total SEY, δ_{tot} , is a sum of two quantities: i) a true SEY and ii) a component which is a multiplication of incident electron energy dependent elastic reflectivity, δ_{Elastic} (which $\rightarrow 1$ as the incident electron energy $\rightarrow 0$) and the probability for elastic reflection in the limit of zero primary electron energy, R_0 . The sum is given by [6 (page 14), 7, 21],

$$\delta_{\text{tot}}(E_e, \theta) = \delta_{\text{true}}(E_e, \theta) + R_0 \delta_{\text{Elastic}}(E_e) \quad (1).$$

The true secondary yield for perpendicular incidence can be expressed by a universal function [21] that is characterized by two material parameters δ_{Max} and ε_{Max} ,

$$\delta_{\text{true}}(E_e, \theta) = \delta_{\text{Max}}(\theta) \frac{sE_e / \varepsilon_{\text{Max}}(\theta)}{s - 1 + [E_e / \varepsilon_{\text{Max}}(\theta)]^s} \quad (2)$$

where,

$$\delta_{\text{Max}}(\theta) = \delta_{\text{Max}}^* \exp\left[\frac{1}{2}(1 - \cos(\theta))\right] \quad (3)$$

$$\varepsilon_{\text{Max}}(\theta) = \varepsilon_{\text{Max}}^* [1 + 0.7(1 - \cos(\theta))] \quad (4)$$

$$\delta_{\text{Elastic}}(E_e) = \left(\frac{\sqrt{E_e} - \sqrt{E_e + E_0}}{\sqrt{E_e} + \sqrt{E_e + E_0}} \right)^2 \quad (5)$$

In the above equations the quantities E_e , δ_{Max} , ε_{Max} and θ , are the incident electron energy, the maximum of δ_{true} , the incident electron energy at δ_{Max} , and the angle of incidence of the primary electrons ($\theta = 0$ implies perpendicular impact), respectively. $E_0 = 150$ eV is a fit parameter to the measured elastic reflection of electrons and $s \approx 1.35$ (a value of 1.35 has been determined for fully conditioned copper [22] and s is constraint to be > 1). The quantity R_0 (in the range of 0 to 1) in this model accounts for the enhancement of the EC build up during the passage of a bunch train by the preceding bunch/bunch-train. Thus, R_0 acts as a memory effect for the EC build up inside the vacuum chamber even after the bunch train has passed by.

Table I lists the EC simulation parameters for the PS. Primary seed electrons are assumed to be produced by gas ionization. In our simulations we varied the gas ionization cross section by about 50% to investigate its effect on the steady-state values of EC line-density. This study showed that the EC steady-state condition has a very small dependence ($< 1\%$) on the ionization cross section for our beam and chamber parameters. The PS EC detector is located in an elliptical 316LN (low carbon with nitrogen) stainless steel chamber. Test-bench measurement data on the 316LN stainless steel [23] have been

fitted to the universal function given by Eq. (2) which gave $\delta_{\text{Max}}^* = 1.85$, $\varepsilon_{\text{Max}}^* = 282$ eV and $s=1.513$. These values are probably too pessimistic, because it has been shown that [7] the scrubbing reduces SEY. In the case of PS several years of beam operation certainly had scrubbing effect. Therefore, we have carried out simulations searching for a somewhat reduced δ_{Max}^* in the range of 1.3 to 1.7 which best represents our measurement data.

TABLE I. PS machine and EC parameters used in the ECLLOUD and PyECLLOUD simulations.

Parameters	Values
Proton Momentum [GeV/c]	26
Number of Bunches/turn	72
Bunch Intensity	1.36E11ppb
Bunch spacing [ns]	Varying (25-50)
Bunch Length	Varying
Bunch Shape/Profiles	Varying shapes
Kicker Gap [μs]	0.3
Beam Pipe:	
H and V Aperture (half) [cm]	7.3 (H), 3.5 (V)
Material of the Beam Pipe	Stainless Steel 316 LN
Beam Transverse Emit. ($\varepsilon_x = \varepsilon_y$) [μm]	2.1
Lattice Function at the Detector	
β_x and β_y [m]=	22.14, 12.06
Ionization Cross section [Mbarn]	1 and 1.5
Gas Pressure [nTorr]	10
Maximum SEY yield δ_{Max}^*	1.57 ^a (1.3-1.7)
Parameter s in Eq. (2)	1.35 ^{a,b} (1.282- 1.513)
R_0 : Probability for Elastic	
Reflection in the Limit of Zero	
Primary Energy of Electrons	0.55 ^a (0.3-0.7)
$\varepsilon_{\text{Max}}^*$ Electron Energy at δ_{Max}^* [eV]	287 ^a (230-332)

^a Best set of SEY parameters from the current study.

^b $s=1.513$ gives the best fit to the bench test SEY data on a Stainless Steel 316 LN sample. But the current PS EC data suggests $s \approx 1.35$.

TABLE II. HL-LHC machine parameters and EC parameters used in the ECLLOUD and PyECLLOUD simulations.

Parameters	Values
Proton Energy [GeV]	7000
Number of Bunches/turn	2808 @ 25ns bunch spacing (Nominal: 2808 @25ns bunch spacing) 1404 @ 50ns bunch spacing
Bunch Intensity	2.2×10^{11} ppb @ 25ns bunch spacing 3.5×10^{11} ppb @ 50ns bunch spacing (Nominal: 1.15×10^{11} @25ns bunch spacing[2])
Bunch spacing [ns]	25 and 50
Bunch Length	Varying
Bunch Shape/Profiles	Varying shapes
LHC RF (frequency and RF Voltage)	400 MHz, 16 MV (max.)(Main rf system) 800 MHz, 8 MV ^a (max.)
Kicker Gap [ns]	200
Beam Pipe: H and V half Aperture [cm]	2.2 (H), 1.73 (V)
Material of the Beam Pipe,	
Warm sections	TiZrV Non-evaporable Getter (NEG)
Cold sections	Saw Tooth shapes
Beam Transverse Emit. ($\varepsilon_x = \varepsilon_y$) [μm]	2.5 for 25 ns bunch spacing 3.0 for 50 ns bunch spacing
Peak Virtual luminosity [$(\times 10^{34} \text{cm}^{-2} \text{s}^{-1})$]	24 @ 25 ns bunch spacing 25 @ 50 ns bunch spacing (Nominal: 1 @ 25 ns bunch spacing [2])
Leveled pk luminosity [$\times 10^{34} \text{cm}^{-2} \text{s}^{-1}$]	7.4 @ 25 ns bunch spacing 3.7 @ 50 ns bunch spacing
Ave. Lattice Function β_x and β_y [m]=	86.37, 92.04
Source of primary electrons	100% Photo emission
Reflectivity	20%
Reflected electron Distribution	$\cos^2 \psi$
Maximum SEY yield δ_{Max}^*	1.3 to 1.7
Parameter s in Eq. (2)	1.35
R_0 : Probability for elastic reflection in the limit of zero primary energy of electrons	0.2 to 0.7
$\varepsilon_{\text{Max}}^*$ Electron energy at δ_{Max}^* [eV]	239.5

^a Foreseen Landau cavity [14].

For most part of the PS cycle the measured EC build up in the experiment [16] was in a steady-state condition (because, the rf manipulation was relatively slow compared to the

EC growth and its decay per passage), except during the fast bunch rotation. In order to guarantee that a steady-state condition is reached in our simulated EC build up, it was necessary to carry out calculations for multiple turn of the PS bunch train taking into account the filling pattern, kicker gap and details of bunch profiles. In some instances, we were required at least fifteen passages to observe reach of EC steady-state. All of our PS simulations were carried out for twenty passages through the EC detector. This gives enough safety margins (see Sec. III B for details).

In case of the HL-LHC the EC simulations have been carried out using the parameters listed in Table II. We assume that the primary seed electrons are exclusively due to the synchrotron-radiation induced photo-emission from the inner beam-pipe surface. In the model, about 80% of the photons produce photo-electrons when they first impact the beam pipe. All of these electrons lie in a narrow cone of 11.25° and, in a strong dipole field, will never get much accelerated by the field of the proton beam. Consequently, they will not contribute to further EC build up. On the other hand, the photo-electrons produced by the remaining 20% of the photon flux are taken to be distributed azimuthally according to $\cos^2 \psi$ and some of these contribute to the further EC build up in the LHC dipoles.

III. E-CLOUD MEASUREMENTS AT CERN PS

A. Experiment

Current PS e-cloud measurements have been carried out using the PS EC detector. Until 5 ms before the beam extraction the rf manipulations was similar to the LHC25. By this time, the final train of 72 bunches with 25 ns bunch spacing was fully formed. The rf voltage of the 40 MHz rf system was programmed to be at 40 kV. Then new rf manipulation sequences have been adopted as shown in Fig. 3(a). The 80 MHz rf system was turned on with a rf phase either at 0° (in phase) or 180° (counter phase). From here on, five different iso-adiabatic bunch manipulation schemes have been followed. 1) Voltage on the 40 MHz rf system has been increased linearly from 40 kV to 100 kV, keeping the 80 MHz rf system turned off. This left the bunches in a single harmonic (SH) rf bucket and the bunches were continuously being shortened for the next 5 ms (black curve in Fig. 3(b)). 2) BSM50: the 40 MHz and 80 MHz rf systems have been ramped up simultaneously in phase from 40 kV to 100 kV and 0 kV to 50 kV, respectively. Here the beam has been maximally squeezed giving rise to the shortest bunch and the final value of $V_2(80\text{MHz})/V_1(40\text{MHz})=0.5$. 3) BSM25: similar to “2” but 80 MHz system ramped only up to 25 kV, 4) BLM25: similar to “3” but, the two rf systems in counter phase and 5) BLM50: similar to “2” but, rf systems in counter phase. The last rf manipulation led to nearly “flat” bunches.

Figure 3(b) shows the ESME simulated RMS bunch lengths in the PS for the entire rf cycle of interest for a 0.26 eVs bunch. It is important to note that the rf voltage ratios $V_2(80\text{MHz})/V_1(40\text{MHz})$ were varying from zero to a set final value of ± 0.50 during the 5 ms of the rf manipulation until the beam get ejected. Ideally, we wanted to hold the beam at the final values of the voltage ratios for an extended period. Operational constraints on the LHC25 cycle during the time of the experiment prevented us to extend.

Figure 4 shows the measured bunch profiles using the PS wall current monitor (and the tomoscope application program) for the region where EC build up is observed. The PS beam intensity for the three cases shown here was about 980×10^{10} protons/72 bunches (which is about 20% larger than that used in Ref. 16) and the measured RMS transverse emittance (inferred by wire scanners) was about $2.1 \mu\text{m}$. A total of 140 traces with delay of 480 PS revolution periods from trace to trace were recorded. The trace number and the corresponding time on the PS cycle relative to the beam ejection are listed in Table III. Data show that bunch profiles for trace-95 to trace-130 in all three cases mentioned above resemble one another except for a small difference arising from the beam intensity variation (<1%). Trace-135 to Trace-140 correspond to the last 5 ms and differ significantly.

TABLE III. Trace number versus time relative to the beam ejection from the PS. These are referred to in Fig. 5.

Trace	Time Relative to PS Beam Ejection (ms)	Comments
Trace95	-46.30	No EC (Background)
Trace104	-36.24	No EC (Background)
Trace109	-31.21	Start of EC
Trace115	-25.17	Growth pt.(Mid)
Trace120	-20.13	Stable EC
Trace130	-10.07	Same as Above
Trace135	-5.03	40MHz \oplus 80MHz
Trace136	-4.03	„
Trace137	-3.02	„
Trace138	-2.01	„
Trace139	-1.01	„
Trace140	0 ^a	„

^aThe fast bunch rotation were removed from the rf cycle on LHC25 during these dedicated experiments

Figure 5(a) displays typical bunch profiles at beam ejection for all five cases studied here. The RMS bunch lengths in each case have also been listed for comparison. Figure 5(b) shows a typical PS bunch train of 72 bunches at ejection.

Figure 6 presents typical EC monitor scope data over the last 40 ms on the PS cycle for BLM50 and data over the last 10 ms for the SH and BSM50 cases. Figure 7 shows the EC line density from BPU1 for each of the PS turns with a bunch profile shown in Fig. 4. The data show that the first observable EC signal above the background noise was seen at Trace109. Since the rf manipulations are sufficiently slow (i.e., the incremental change in bunch profile is almost negligible for a number of passages through the EC detector

region as compared with EC growth and decay time), one can assume that the EC line density has reached a steady-state in all cases shown in Fig. 7. It is evident that the growth and steady-state values of EC line-density strongly depend on the bunch profiles. However, independent of their peak electron-line density each one will decay in about 0.1 μ s after passage of the last bunch.

B. EC Simulations and Comparison with the Data

The simulation studies of the measured EC build up in the PS have been carried out using the code ECLLOUD as well as PyECLLOUD. The simulation results from these two are quite consistent. Here we present the results only from the simulations carried out using the latter code.

Starting from the measured values of $\delta_{\text{Max}}^* = 1.85$ and $\varepsilon_{\text{Max}}^* = 282$ eV for the 316LN stainless steel, we scanned the SEY parameter space shown in Table I. All of our simulations take the exact bunch profiles into account (for example profiles shown in Fig. 4) with bunch to bunch intensity variation similar to that shown in Fig. 5(b) and the measured beam intensity in the PS. Figure 8 illustrates an example of such simulation results for two sets of SEY parameters and for three different beam profiles SH, BSM50 and BLM50 cases at ejection. Figure 8(a) displays reach of steady-state with about ten passages of the beam train. However, the predicted EC line density is about four orders of magnitudes smaller for the BLM50 as compared to the other two cases which contradicts the measurements (see for example EC line-density for trace140 for these three cases in Fig. 7 a-c). By changing the δ_{Max}^* from 1.55 to 1.57 keeping all other simulation parameter unchanged, we find steady-state is reached at about fifteen passages. Also, the simulated line density for the BLM50 found to approach the measurement data. These simulations clearly show the sensitivity of the EC build up to the bunch profile and the SEY parameters. This suggests that one could possibly use the bunch profile dependence of EC growth to estimate the SEY quite accurately.

By comparing simulated EC line-density with the measurements we tried to find a unique set of SEY parameters which explains all EC data at ejection simultaneously. Figure 9 displays one such comparison for BLM50, BSM50 and SH. The simulations have been performed using $\varepsilon_{\text{Max}}^* = 287$ eV, $\delta_{\text{Max}}^* = 1.57$ and $R_0 = 0.55$. There is no normalization between the simulation results and the measurement data. We find quite a good agreement between the steady-state values for the BSM50 and SH cases. Also, the overall trend is well reproduced. In the case of BLM50 the quality of the agreement is less satisfactory. Here the simulated EC line density grows rather slowly initially and then reaches a steady-state maximum at a level about 40% higher than the measured value. This discrepancy is being investigated. However, even for this case the predicted cumulative number of electrons per turn lies within 30% of the measured value of about 3×10^{12} electrons.

Next, the simulations have been carried out to predict the cumulative EC build up for the last 40 ms using the set of SEY parameters established using ejection data. Figure 10 presents the measured cumulative number of electrons per PS turn versus the relative

time in the PS cycle. Approximately about 10% errors were assigned to the measured data points which include a systematic error in transfer function and a background subtraction error. The three overlaid curves in Fig. 10 represent simulation results with a normalization factor of 0.83. The overall trend of the cumulative electrons is predicted quite well in all three cases. Simulations are found to reproduce even the observed oscillations during the last 5 ms in the case of BLM50. However, for SH and BSM50, the accumulated electrons on the last turn of the beam in the PS are underestimated by 25% and 50%, respectively, in the simulations.

From the PS EC measurements we clearly observe a dependence of EC growth on the bunch profile. The ratios of measured cumulative numbers of electrons at ejection were found to be 2.7 ± 0.4 and 2.3 ± 0.3 for BSM50/BLM50 and SH/BLM50, respectively. Certainly, the BLM gives rise to considerably smaller EC build up than the other two cases. A comparison between measurements and simulations sets a stringent range of values on the SEY parameters at the PS EC detector. For example, we found $\varepsilon_{\text{Max}}^* = 287$ eV ($\pm 3\%$), $\delta_{\text{Max}}^* = 1.57$ ($\pm 8\%$) and $R_0 = 0.55$ ($\pm 3\%$). Moreover, the studies in the PS helped us to benchmark the EC simulation codes and the employed SEY model.

IV. E-CLOUD IN THE HL-LHC

Over the last one and half decades significant research has been carried out on the LHC EC issues [2, 5-8, 11, and 24-27]. Most of the past simulations assumed Gaussian bunch profiles and bunch intensities close to the nominal LHC design values [2]. A considerable effort has been put into scanning the SEY parameter space. Ref. 24 presents EC-simulation results for the higher intensity operation of the LHC including some simulations using flat rectangular profiles of ≈ 38.1 cm bunch length (non-realistic to the current LHC and proposed HL-LHC operating scenarios). Further, all of them have assumed about 25% and 50% larger transverse emittances for the 25-ns and 50-ns bunch filling patterns, respectively, than in the more recent HL-LHC specifications. However, the EC is a very complex, non-linear multi-dimensional phenomenon. Further, the SEY parameters improve with machine operation. As a result of this, it is practically impossible to foresee every issue that one might encounter. In this section, we focus our study on realistic bunch profiles and better established SEY parameters.

Currently, the LHC is not instrumented with EC monitors as in the case of the PS and the SPS at CERN. All the information related to the EC in the LHC is deduced from the measured vacuum activities in various sectors of the ring and from the measured cryo-heat load in the cold arcs. Recently, a stringent range of SEY parameters has been deduced [11] by using the 2011-12 vacuum data in the uncoated warm regions of the LHC and comparing it with ECLOUD simulations, the parameters $\varepsilon_{\text{Max}}^* = 239.5$ eV and $\delta_{\text{Max}}^* < 1.55$ have been inferred. Here, we study the EC for the LHC using the HL-LHC beam parameters and the above values of SEY for a variety of possible realistic bunch profiles resulting from the existing single harmonic 400 MHz rf system and double harmonic rf made of 400 MHz+800 MHz systems, with the goal of investigating if a particular bunch profile is better than another from the point of view of EC mitigation .

Figure 11 shows ESME-simulated bunch profiles for the LHC. Guided by the 2011-2012 measurements on the bunch profiles in the LHC at 4 TeV, we have used a Hofmann-Pedersen (elliptical) distribution for the beam in 400 MHz rf buckets at 7 TeV. An rf voltage of 16 MV is assumed on the LHC 400 MHz rf system. The profiles BSM50 and BLM50 have been generated by superposing the 800 MHz rf wave on the fundamental rf wave of 400 MHz with voltage ratios $V_2/V_1 = \pm 0.5$, respectively. The dashed dark curve corresponds to the bunch profile from a constant beam particle density distribution in the longitudinal phase space, “water-bag” model [28].

EC simulations have been carried out with ELOUD as well as with the PyELOUD using the parameters listed in Table II. We have also extended some of the simulations to the intensity range of 1 to 4×10^{11} ppb. The current simulations use $\varepsilon_{\text{Max}}^* = 239.5$ eV, δ_{Max}^* in the range 1.3 to 1.7 and R_0 in the range of 0.2 to 0.7. We have used a standard SPS batch made of four PS train each separated by 200 ns. For the 50 ns and 25 ns bunch filling pattern a SPS batch had 144 and 288 bunches, respectively and the individual bunch profiles were similar to those shown in Fig. 11. A clear signature of a steady-state is seen by the end of the passage of the first PS batch as shown in Fig. 12 for all values of SEY parameters considered here. Preliminary results from a similar EC simulation for the LHC with different bunch profiles generated using a double harmonic rf system have been reported earlier [29]. The electrons from EC ultimately deposit their energy on the beam pipe. The heat loads on the LHC cryo-system resulting from the deposited energy from the electrons have been deduced.

Cryogenic superconducting dipoles in the LHC occupy about 66% of the ring and carry the majority of the cryo-heat load. Therefore, we concentrate all of our simulations on the LHC dipoles (arcs). The calculated heat load for various bunch profiles and two sets of SEY are shown in Fig. 13(a) and the heat-load dependence on the bunch intensity is shown in Fig. 13(b). The contributions from quadrupoles and other cryo-magnets to the total heat load are ignored here. The dashed-dot line and dotted lines represent current cryo-heatload handling capacity available for EC, calculated using total design capacity reduced by the contributions from the resistive impedance part [24, 26]. These calculations assume a separate upgrade to the LHC triplets cryo-system to handle the heat load from the debris around collision points during the HL-LHC era.

Figure 13(a) clearly shows that the heatload from EC has very little dependence on the bunch profile including that for the water-bag distribution. Therefore, BLM or water-bag distribution will not help as an EC mitigation technique in the LHC.

Simulations show that even for the most pessimistic case of $\delta_{\text{Max}}^* = 1.7$, $R_0 = 0.7$ (from Table II) the average heat load is ≤ 0.8 W/m in the case of the 50 ns bunch filling pattern with 3.5×10^{11} ppb. On the other hand, the calculated heat load for any of the 25-ns bunch filling patterns is more than the design heat-load handling capacity of the LHC cryo-system if $\delta_{\text{Max}}^* \geq 1.5$. Therefore, upgrades to the LHC cryo-system are inevitable for future operation with 25 ns bunch spacing at higher intensities unless the SEY is reduced significantly from the current values. Our simulations demonstrate that the LHC filling

pattern with 50-ns bunch spacing has a clear advantage over the 25-ns bunch spacing even during the HL-LHC era. This is in quite good agreement with the findings of the Ref. 24.

The observed difference between PS and the LHC EC dependence on the bunch profiles may be understood by examining the difference in the bunch length in these two cases. The LHC bunches are about an order of magnitude shorter than those studied in the PS. For example, the shortest bunch in the PS (in our experiment) has a bunch length (4σ) of about 300 cm, while, for the LHC, the longest bunch length contemplated was about 36 cm. To investigate this issue further we extended our simulation studies in the LHC on two types of long bunches with 25 ns bunch spacing filling pattern and, with similar dN/dX at the rising and trailing edges of the bunches as shown by red curve (BLM50) in Fig. 11. In one case we had constant bunch intensity of 2.2×10^{11} ppb and in the other case we kept the peak line density of the protons the same. In both cases the bunch lengths have been varied in the range of 1 ns to 4 ns. (In practice, these long bunches can be produced either by using multiple harmonic rf systems or a wide band barrier rf system. See for example Fig. 3 of Ref. 30.). Figure 14 shows the calculated average heat load as a function of total bunch length for constant bunch intensity. We find that for a given set of δ_{Max}^* and R_0 , there is little dependence of the heat load on bunch length if the LHC bunches are very short or very long. However, one can see that for the bunch lengths in the range of about 1.3 ns to 3 ns there is a significant dependence of heat load as a function of its length for high δ_{Max}^* . And, for low δ_{Max}^* the dependence is much softer. This behaviour of EC needs further investigation. For the case with constant peak intensity the heat load found to grow nearly exponentially with bunch length.

The fact that the EC build up has little dependence on the bunch profiles in the LHC for HL-LHC beam parameters bodes well for the foreseen rf upgrades during the HL-LHC era. The high intensity beam can be made stable by use of a 2nd harmonic 800 MHz Landau cavity if the bunches are in the BSM mode (or BLM mode for longitudinal emittance below some threshold [30]). With the current analysis, we show for the first time that the use of Landau cavity in the LHC will have a negligible effect on the EC growth.

V. SUMMARY

During the HL-LHC era the beam intensity in the LHC is expected to go up at least by a factor of two. This has direct implications on the EC growth and the issues related to the beam instability driven by the dynamics of the electron cloud. Therefore it is important to explore and develop techniques to mitigate EC growth. Fully developed techniques like NEG coatings on the inner surface of the beam pipe in warm sections and a saw tooth pattern on the beam screen inside the cold dipole region have been adopted in the LHC. Many other techniques are under consideration.

Encouraged by the preliminary EC simulation results on flat bunch we conducted an experiment in the PS at its extraction energy, to study the correlation between bunch profiles and the EC build up. Exploiting PS rf capabilities, a variety of possible bunch

profiles, including nearly flat bunches, have been generated and the corresponding EC growth has been studied. EC simulations have been carried out incorporating the measured PS bunch profiles. There was a good agreement between the EC measurements and the simulation results. These studies have enabled us to deduce the SEY parameters for the EC monitor region of the PS as $\varepsilon_{\text{Max}}^* = 287 \text{ eV} (\pm 3\%)$, $\delta_{\text{Max}}^* = 1.57 (\pm 8\%)$ and $R_0 = 0.55 (\pm 3\%)$. We also find that, the nearly flat (BLM50) bunches produce about a factor 2.7 ± 0.4 lower number of cumulative electrons than the bunches that resemble Gaussian or elliptical shapes.

We have then extended similar studies to the HL-LHC beam conditions through simulations, where the bunch lengths were nearly ten times shorter than that in the PS at extraction. We found that for the HL-LHC beam parameters the EC build up is almost independent of bunch profiles. Consequently, the foreseen second harmonic 800 MHz Landau cavity that would shorten bunches and make the beam longitudinally more stable, will not pose any additional EC related problems in the LHC. Nevertheless, EC dependence on the bunch length is still seen only at large values of δ_{Max}^* and at much longer bunch lengths than that under consideration for the HL-LHC.

ACKNOWLEDGMENTS

The authors would like to thank the CERN operation team for their help while conducting the beam experiments in the PS accelerator. One of the authors (CMB) is specially indebted to O. Brüning, G. Arduini, E. Shaposhnikova, R. Garoby, E. Metral, G. Rumolo and S. Gilardoni for their hospitality at CERN and many useful discussions. Also, special thanks are due to Humberto M. Cuna for his help in early stages of simulation studies. This work is supported by Fermi Research Alliance, LLC under Contract No. DE-AC02-07CH11359 with the U.S. Department of Energy, US LHC Accelerator Research Program (LARP) and Coordinated Accelerator Research in Europe – High Intensity, High Energy, Hadron Beam (CARE-HHH).

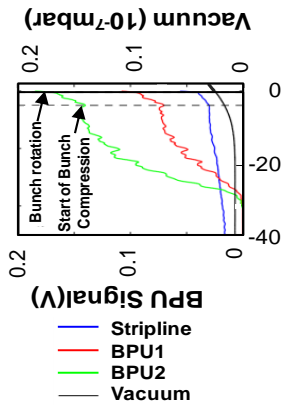
REFERENCES

- [1] O. Brüning and F. Zimmermann, "Parameter Space for the LHC Luminosity Upgrade", IPAC'12 New Orleans, p. 127, <http://accelconf.web.cern.ch/accelconf/IPAC2012/papers/moppc005.pdf>
- [2] "LHC Design Report – Vol. I", edited by O. S. Brüning et al., Chapter-5 in CERN-2004-003-V-1. - Geneva : CERN, 2004.
- [3] G. Budker, G. Dimov, and V. Dudnikov, in *Proceedings of the International Symposium on Electron and Positron Storage Rings, Saclay, France, 1966* (Saclay, Paris, 1966), Article No. VIII-6-1.
- [4] K. Ohmi, Phys. Rev. Lett. **75**, 1526 (1995); M. Izawa, Y. Sato, and T. Toyomasu, Phys. Rev. Lett. **74**, 5044 (1995).
- [5] F. Zimmermann, Phys. Rev. ST Accel. Beams **7**, 124801 (2004).

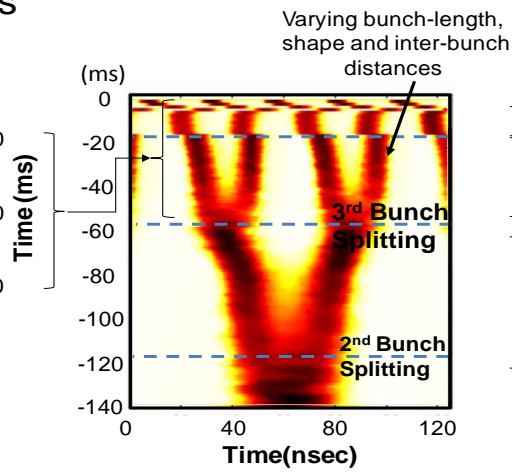
- [6] “Electron Cloud Effects in Accelerators”, edited by K. Ohmi and M. Furman (2004), ICFA Beam Dynamics Newsletter, Vol.33 April 2004, p 14-156.
- [7] R. Cimino, I. R. Collins, M. A. Furman, M. Pivi, F. Ruggiero, G. Rumolo and F. Zimmermann, *Phy. Rev. Letts.* V93. 014801 (2004).
- [8] “Electron Cloud In the LHC,”(Giovanni.Rumolo@cern.ch and frank.zimmermann@cern.ch) <http://ab-abp-rlc.web.cern.ch/ab-abp-rlc-ecloud/>
This site also, lists references to major e-cloud conferences proceedings.
- [9] G. Rumolo, et al, “Electron cloud observations in LHC,” IPAC2011 (2011) p 2862
- [10] “The SPS as a vacuum test bench for the electron cloud studies with LHC type beams,” G. Arduini et. al., PAC2001 (2001) p 685; “Electron cloud studies and beam scrubbing effect in the SPS,” J.M. Jimenez, et. al., LHC Project Report 634, 2003.
- [11] O. Dominguez, et al, IPAC2012 (2012) p 3105.
- [12] E. Shaposhnikova, et al., IPAC2011 (2011) p 211.
- [13] T. Bohl, et al., EPAC98, (1998) p 978.
- [14] E. Shaposhnikova and E. Jensen (private communications, 2012).
- [15] G. Rumolo, Private communications (2011).
- [16] E. Mahner, T. Kroyer and F. Caspers, *Phys. Rev. ST Accel. Beams* 11, 094401 (2008).
- [17] S. Hancock, P. Knaus, M. Lindroos, “Tomographic Measurements of Longitudinal Phase Space Density”, EPAC’98, p 1520;
<http://tomograp.web.cern.ch/tomograp/>
- [18] J. Maclachlan, ESME – longitudinal beam dynamics code.
<http://www-ap.fnal.gov/ESME/>
- [19] Main contributors to the code E-CLOUD were F. Zimmermann, O. Brüning, X.-L.Zhang, G. Rumolo, D. Schulte, and G. Bellodi; E-CLOUD code has been modified by C. M. Bhat in 2011 to handle complex bunch profiles.
- [20] G. Iadarola, “Py-Ecloud and buildup simulations at CERN,”(Presented at E-CLOUD12, June 5-9, 2012, La Biodola, Isola d’Elba, Italy)
<http://agenda.infn.it/conferenceOtherViews.py?view=standard&confId=4303>).

- [21] M. Furman, G. Lambertson, “The Electron-Cloud Instability in the Arcs of the PEP-II Positron Ring,” Proc. MBI97 Tsukuba (1997); M. A. Furman and M.T. F. Pivi, Phys. Rev. ST Accel. Beams **5**, 124404 (2003).
- [22] V. Baglin, I. Collins, B. Henrist, N. Hilleret, G. Vorlaufer, A Summary of Main Experimental Results Concerning the Secondary Electron Emission of Copper, LHC-Project-Report-472. These authors found $s=1.39$ for as received, and 1.35 for fully conditioned copper.
<http://cdsweb.cern.ch/record/512467/files/>
- [23] M. Taborelli, (Test-bench measurements on SEY on 316LN_0 Cmm2), (Private communications, 2012).
- [24] H. Maury, J. G. Contreras and F. Zimmermann, Phys. Rev. ST Accel. Beams **15**, 051001 (2012).
- [25] F. Zimmermann, .A Simulation Study of Electron-Cloud Instability and Beam-Induced Multipacting in the LHC, CERN LHC Project Report 95 (1997); O. Brüning, Simulations for the Beam-Induced Electron Cloud in the LHC beam screen with Magnetic Field and Image Charges,. CERN LHC Project Report 158 (1997); G. Rumolo, F. Ruggiero, F. Zimmermann, Simulations of the Electron Cloud Build Up and its Consequences on Heat Load, Beam Stability and Diagnostics,. PRST-AB **4**, 012801 (2001); F. Zimmermann, Electron Cloud Simulations: An Update, Proc. Chamonix 2001, CERN-SL-2001-003 DI (2001).
- [26] M. A. Furman and V. H. Chaplin, Phys. Rev. ST Accel. Beams **9**, 034403 (2006).
- [27] G. Rumolo and G. Iadarola, “Observations and predictions in the LHC and SPS,”(Presented at E-CLOUD12, June 5-9, 2012, La Biodola, Isola d'Elba, Italy) <http://agenda.infn.it/conferenceOtherViews.py?view=standard&confId=4303>.
- [28] Water-bag distributions for the beam bunches are known to provide single as well as multi-bunch stability against Landau damping. An experiment is proposed in the LHC to confirm beam stability issues (A. Burov et. al., private communications, 2012).
- [29] C. M. Bhat and F. Zimmermann, IPAC2011 (2011) p 1879.
- [30] “Flat bunch creation and acceleration: A possible path for the LHC luminosity upgrade” (2009), C. M. Bhat, FERMILAB-CONF-09-243-AD-APC, the *Proceedings of CARE- HHH workshop 2008 Scenarios for the LHC upgrade and FAIR*, CERN), 2009, CERN-2009-004, 2nd July 2009, p 106-114.

e-Cloud Signals

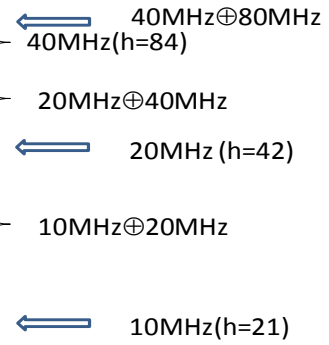


(a)



(b)

PS RF Systems



(c)

FIG. 1 The region of interest from EC point of view in the PS beam on the LHC25 cycle (for four + one bunches out of seventy two). (a) Measured EC signals from BPU1 (red curve), BPU2 (green curve) and stripline (blue curve) detectors along with vacuum (black curve) [16] (b) water-fall plot of one PS bunch out of six, collected using tomoscope, and (c) used PS rf systems for beam quadrupole splitting. The lateral displacement of the bunches in “b” during the last 15 ms is an artifact of triggering the scope and is not real.

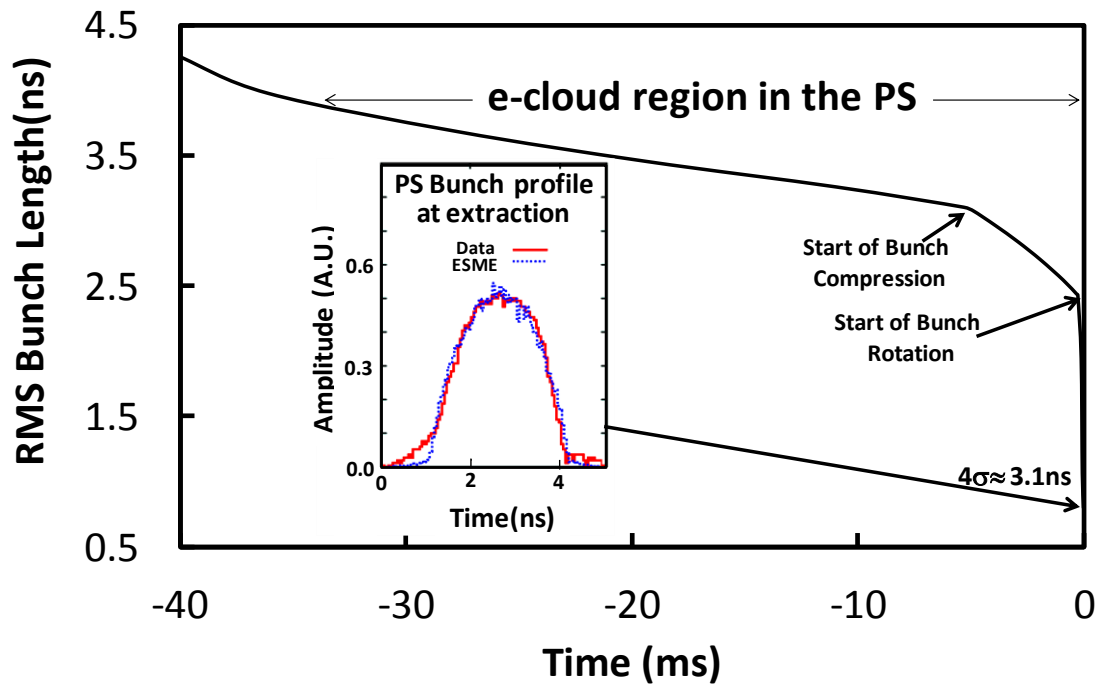


FIG. 2. ESME simulated RMS bunch length variation from -40 ms to 0 ms on the PS-LHC25 beam cycle. The measured bunch profile just before ejection from the PS and its comparison with the predicted bunch profile using ESME is shown in the inset.

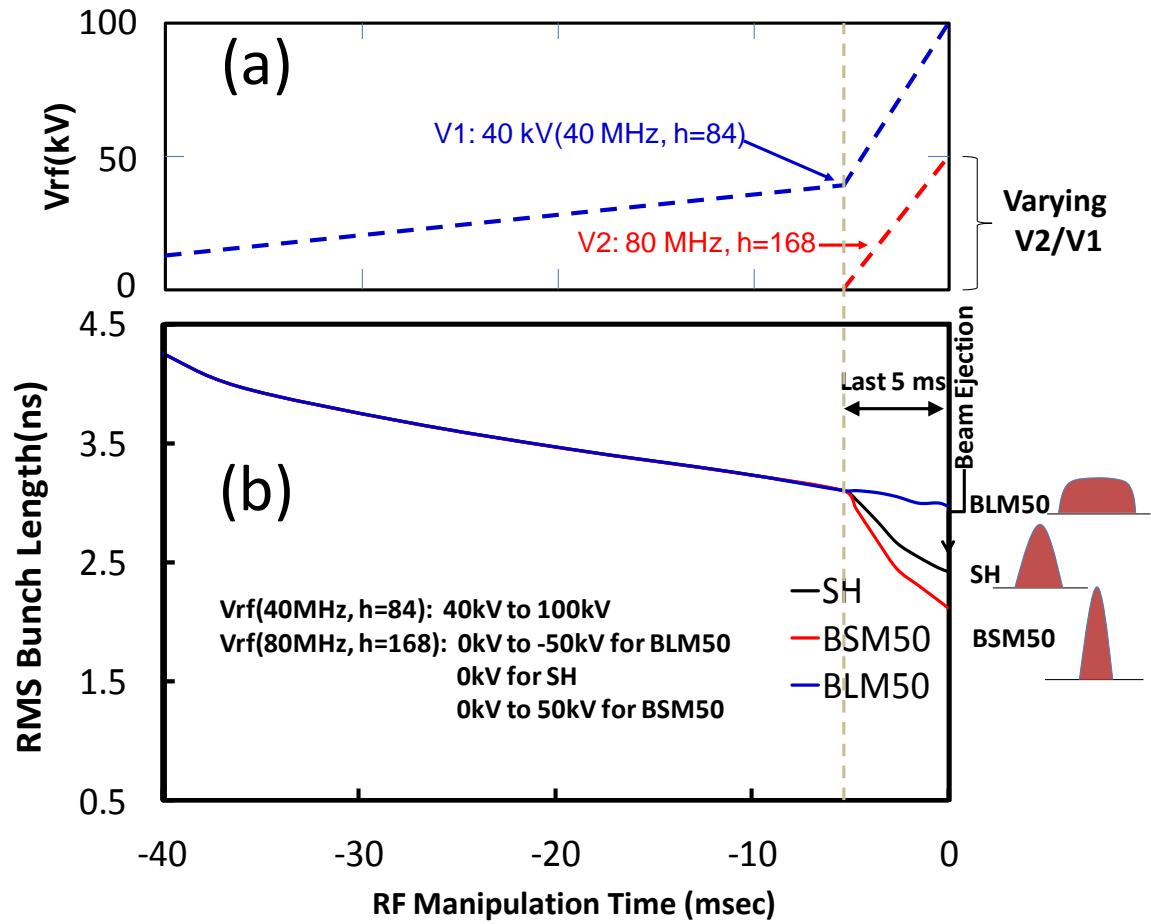


FIG. 3. (a) Schematic of PS rf manipulation and (b) ESME predicted bunch length variation during the last -40 ms to 0 ms in the current experiment. From -40 ms to -35 ms the rf manipulations and bunch length variation are identical to that in Fig. 2 . For the last 5 ms, the 40 MHz and 80 MHz rf systems are ramped up simultaneously and linearly, to final values of 100 kV and 50 kV, respectively.

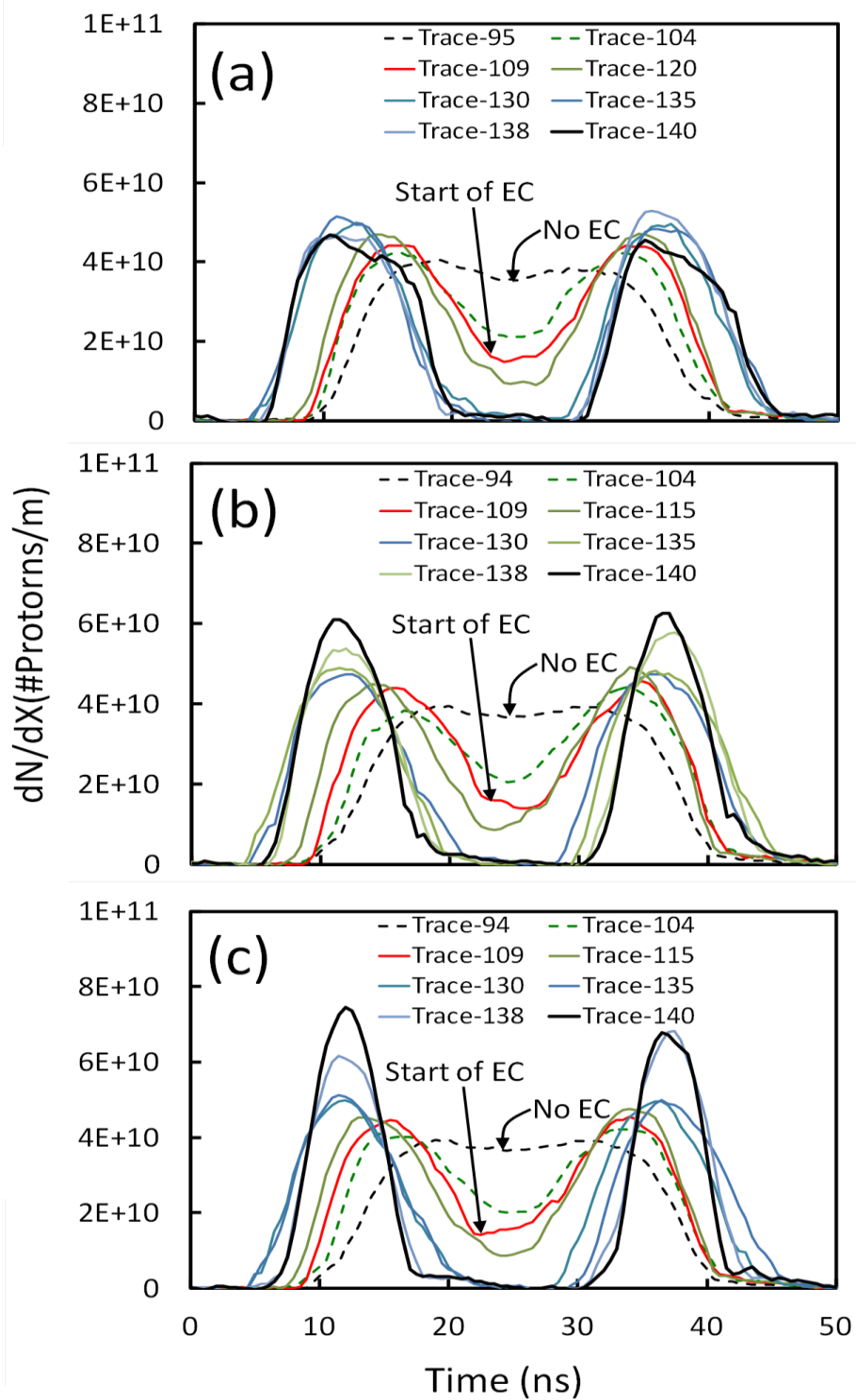


FIG. 4. PS bunch profiles during the last 46.30 ms of the rf manipulations with 20 MHz, 40 MHz and 80 MHz rf systems for a) BLM50, b) SH and c) BSM50 for two bunches out of 72. The rf manipulations differ only during the last 5 ms in these three cases. The trace numbers and the relative time are listed in Table III. The start point of EC build up are also shown.

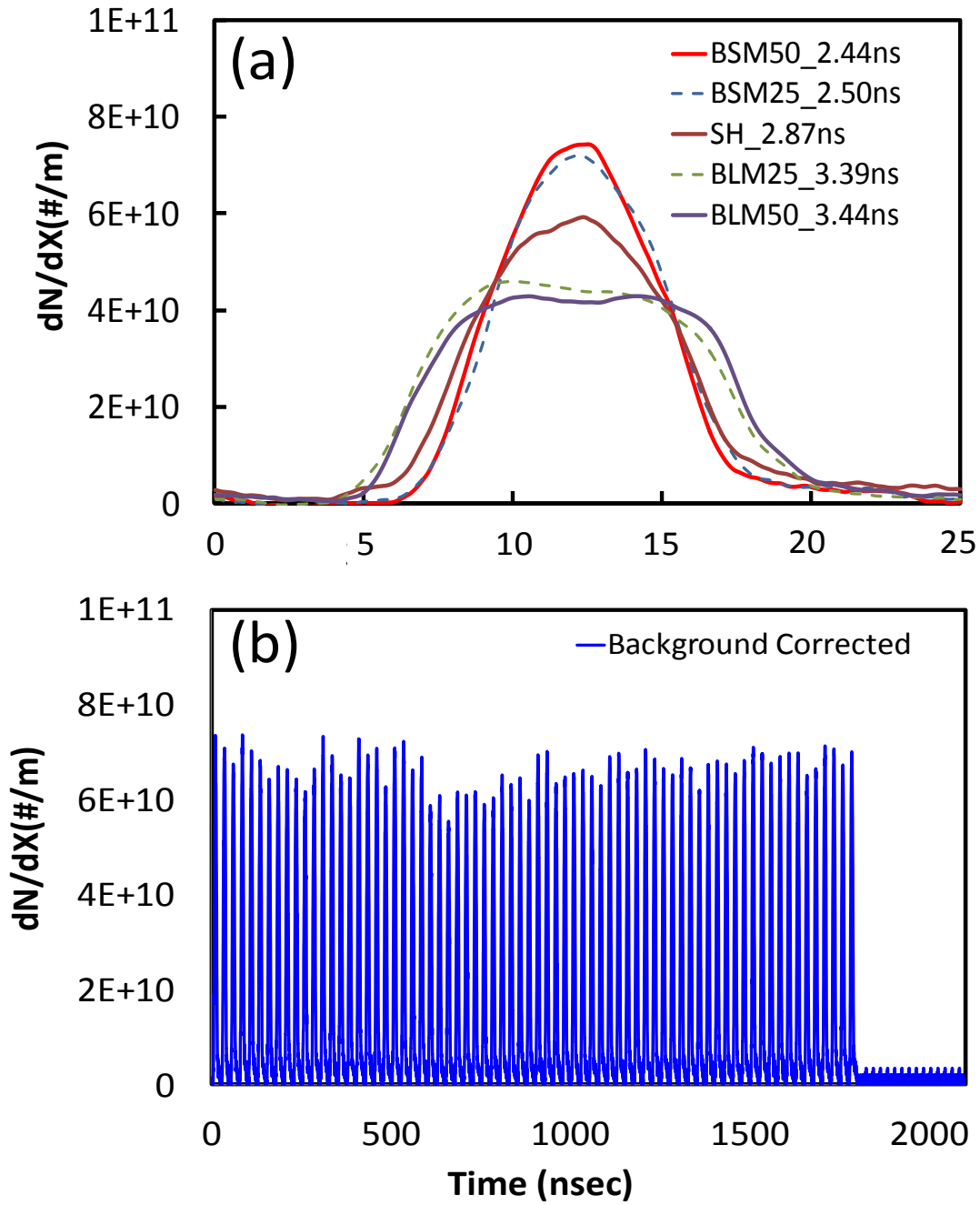


FIG. 5. Typical measured PS bunch profile at ejection for a) all five cases studied here b) a train of 72 bunches with 25 ns bunch spacing (after background correction). The average bunch intensity was $\approx 1.36 \times 10^{11}$ ppb.

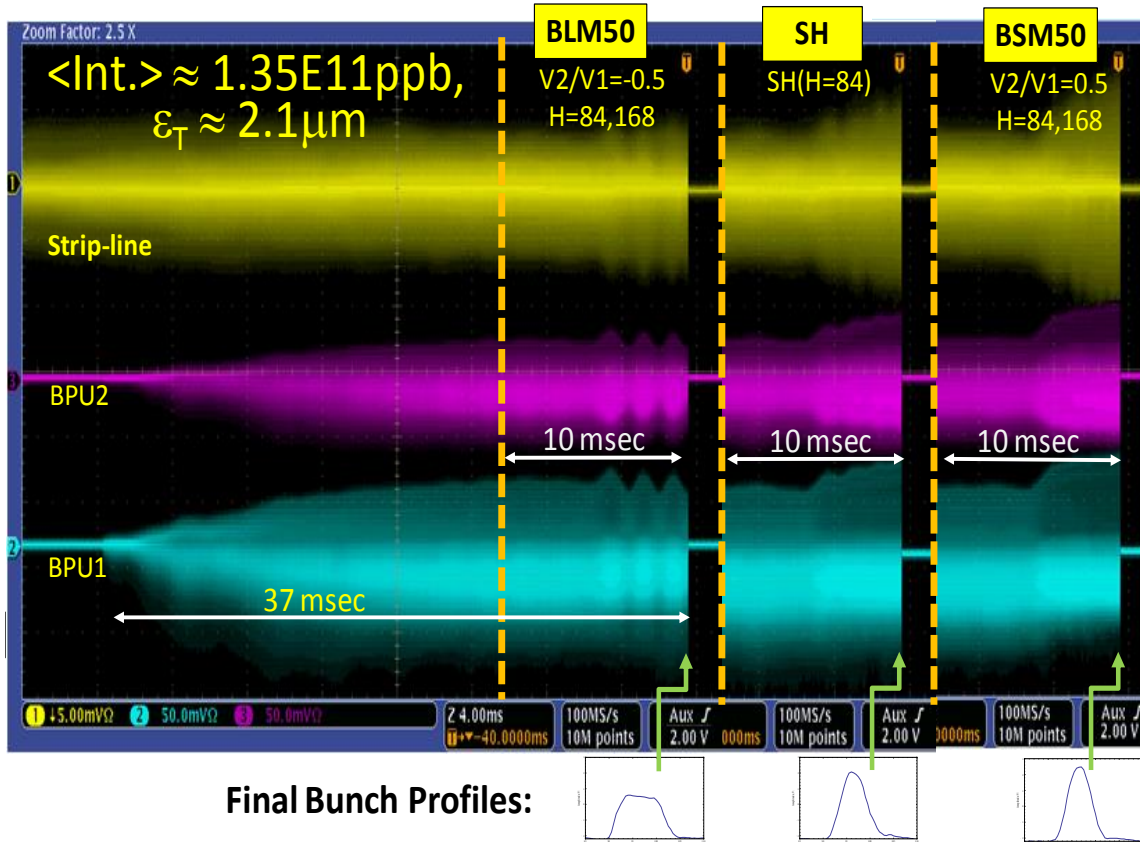


FIG. 6. Signals from the EC monitor from three different detectors viz., strip-line, BPU1 and BPU2 for three rf manipulation scenarios. The bunch shapes at ejection are also shown.

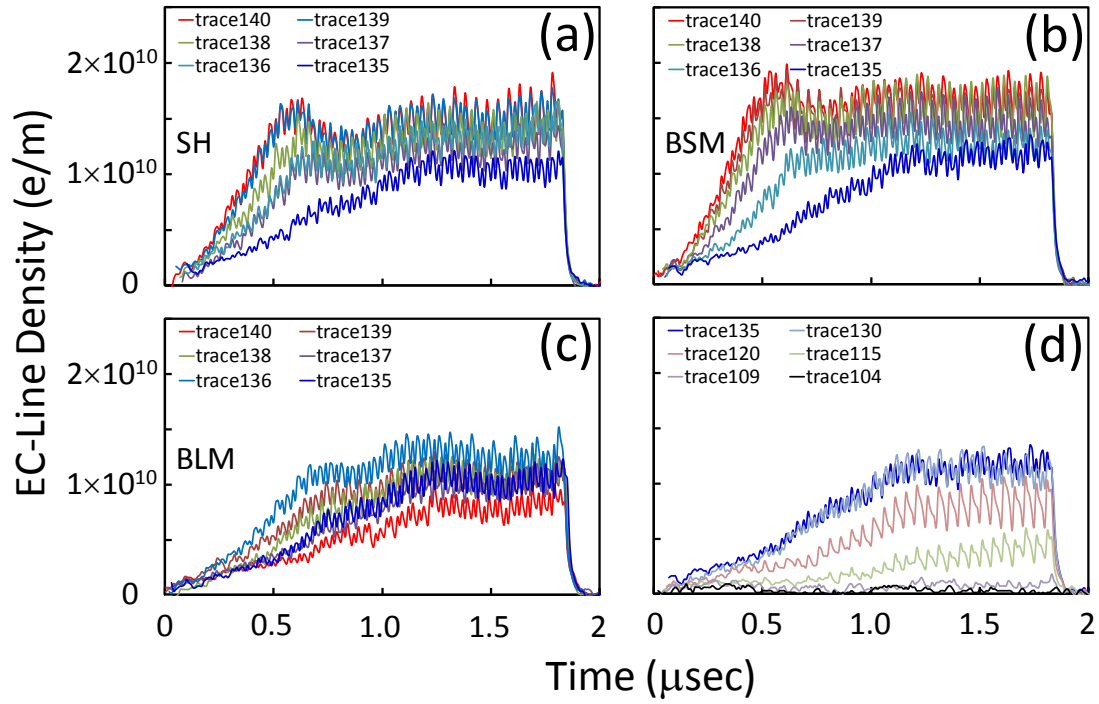


FIG. 7. EC line-density measured at different time of the PS cycle during the last 40 ms before the beam ejection. The data shown are from BPU1 and for the last 5 ms for a) SH, b) BSM50, c) BLM50 and d) data for the first 35 ms. All three cases, SH, BSM50 and BLM50 display similar behavior from 40 ms to 35 ms before ejection as shown in “d”.

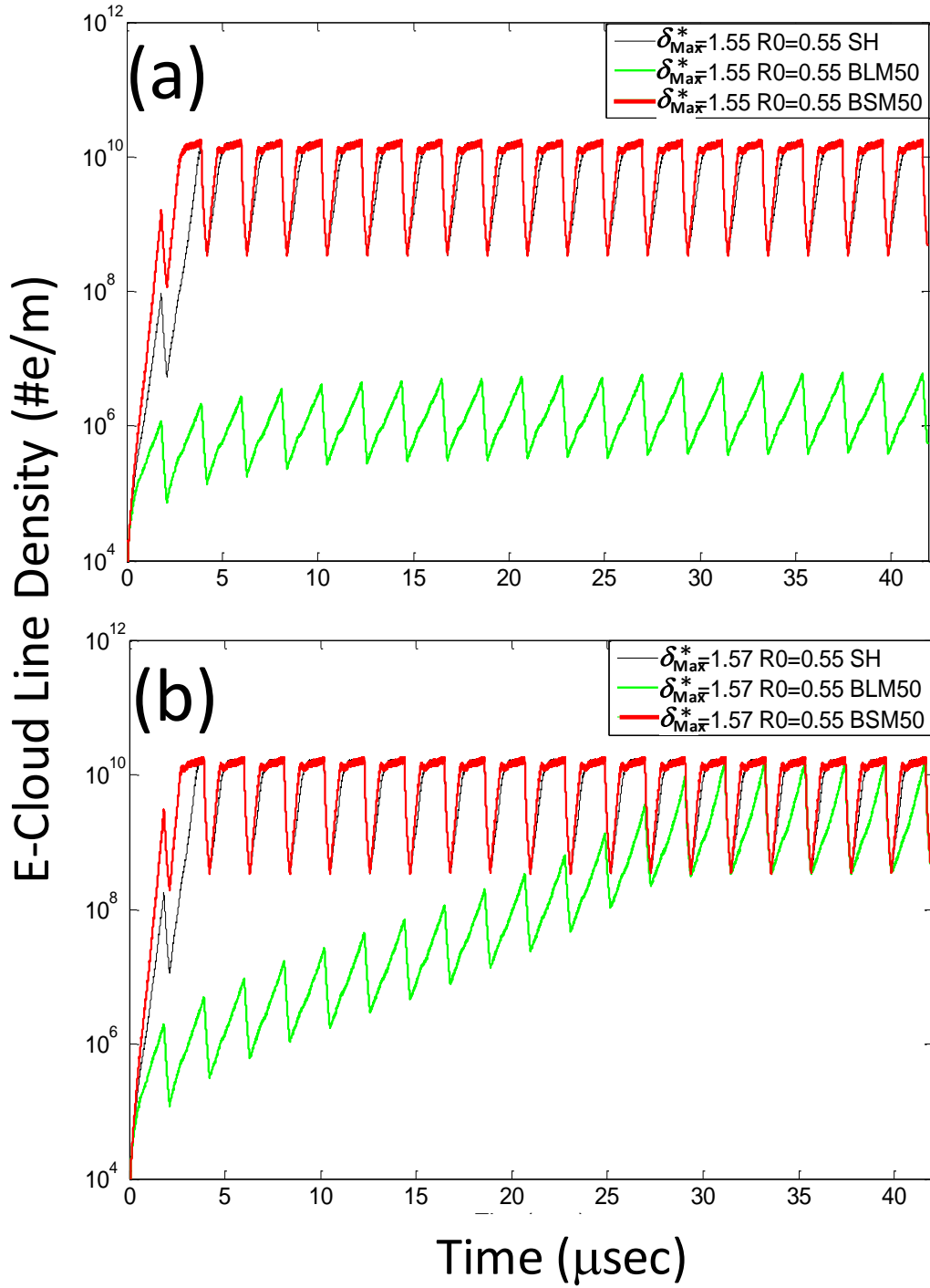


FIG. 8. PS EC simulations using PyECLLOUD with $\varepsilon_{\text{Max}}^* = 287$ eV and a) $\delta_{\text{Max}}^* = 1.55$, $R_0 = 0.55$; b) $\delta_{\text{Max}}^* = 1.57$, $R_0 = 0.55$ (optimized). Calculations are carried out for the drift section of the PS EC detector. These two cases are shown as examples to illustrate the combined sensitivity of EC growth on the SEY parameters and on the bunch shape.

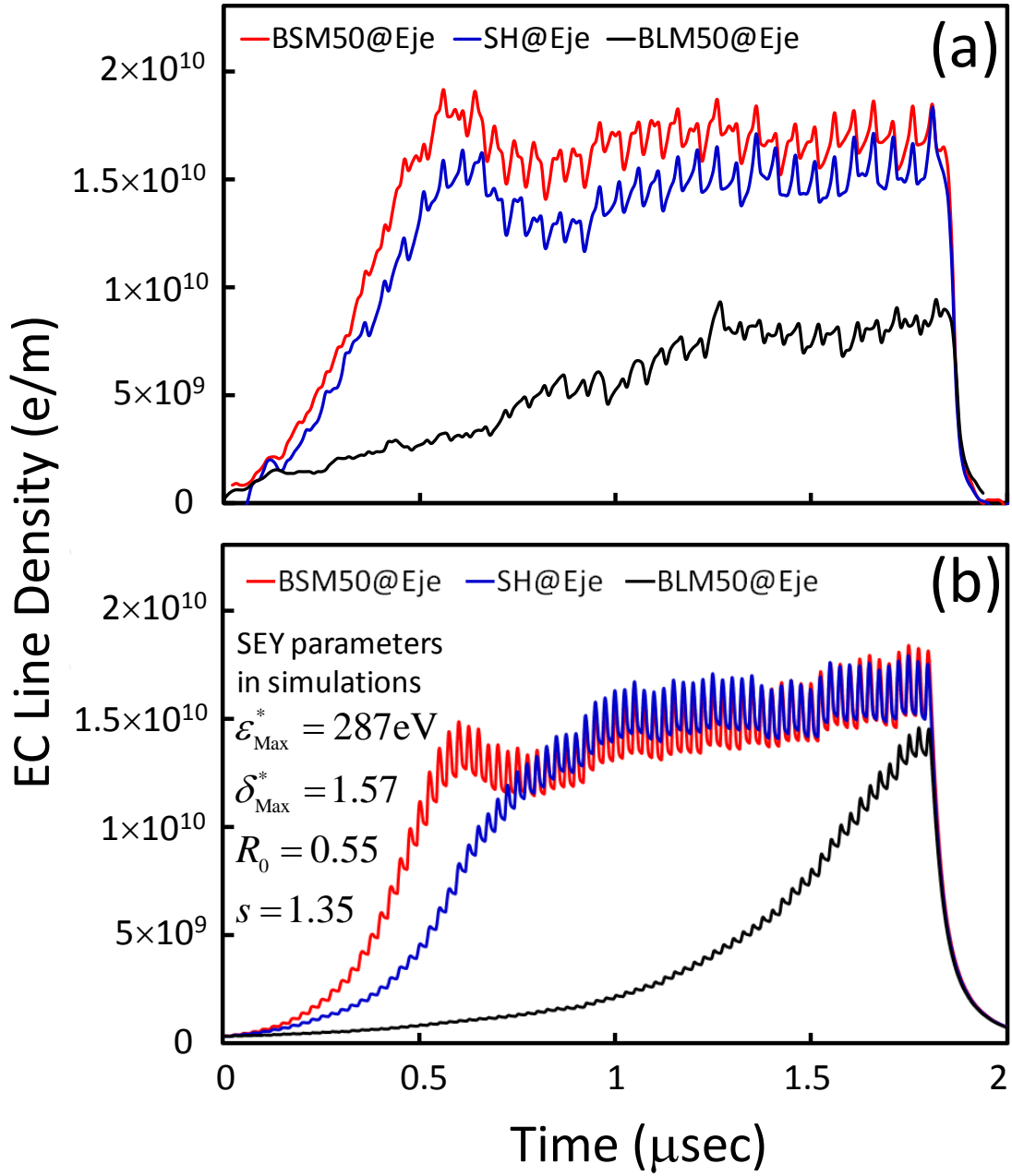


FIG. 9. (a) Measured EC line-density in the PS at ejection and (b) the PyECLOUD simulation results corresponding to the cases shown in “a”.

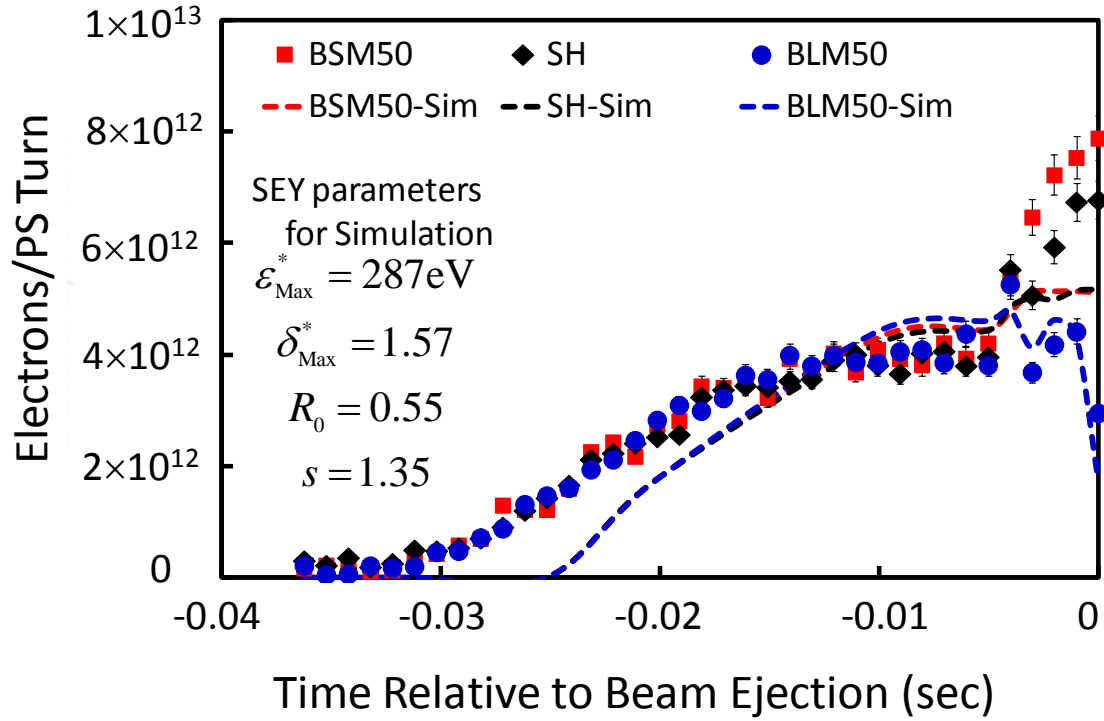


FIG. 10. Overlay of the measured cumulative electrons/PS turn (red squares: BSM50; dark diamonds: SH; and blue circles: BLM50) and the predictions by PyECLoud.

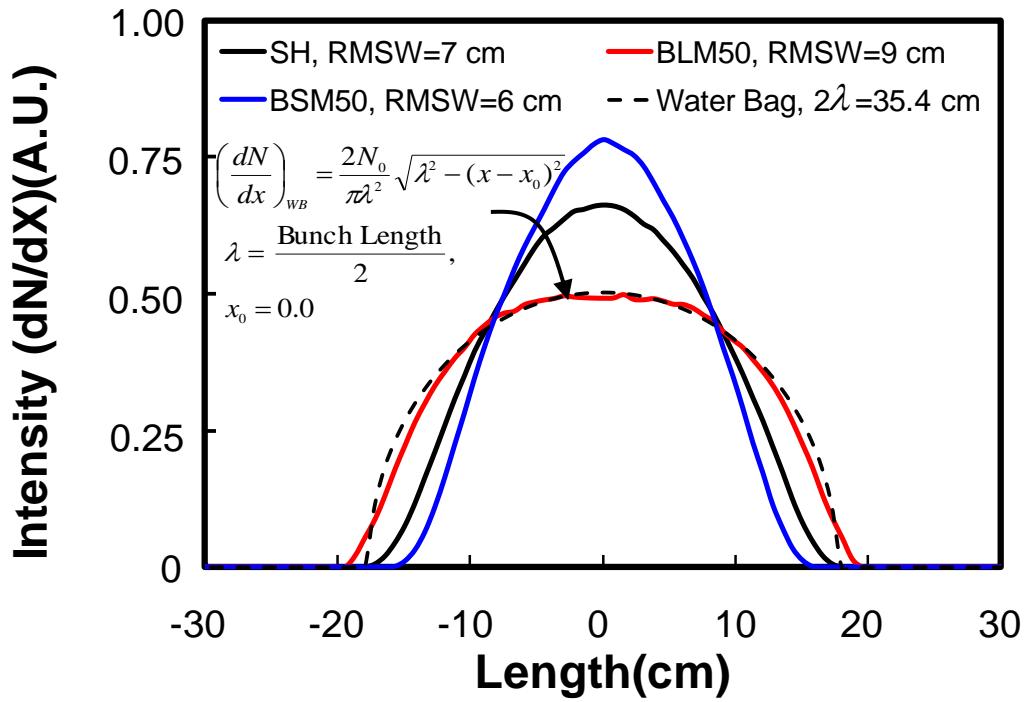


FIG. 11. (ESME) Simulated HL-LHC beam bunch profiles for SH (in 400 MHz rf bucket), BSM50, BLM50 and water-bag. The analytical formula used for the water-bag is also shown.

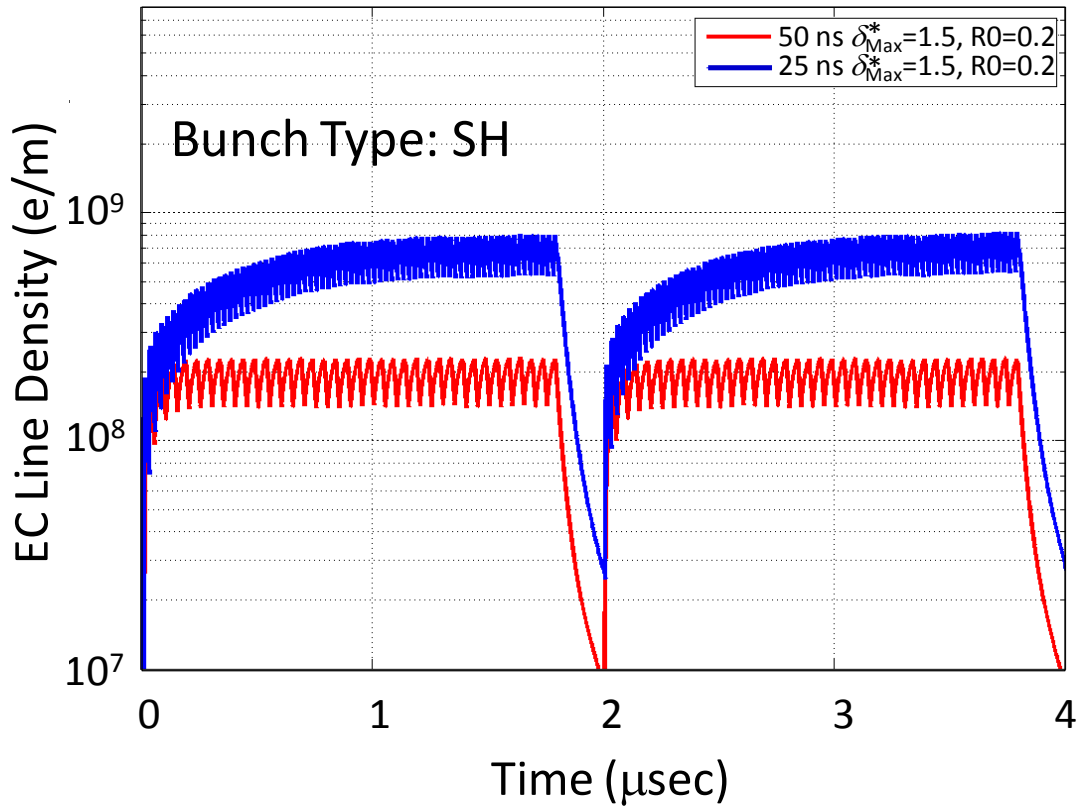


FIG. 12. PyECLoud simulations with $\varepsilon_{\text{Max}}^* = 239.5$ eV for the HL-LHC beam parameters for two PS batches. Red and blue curves are for 3.5×10^{11} ppb with 50 ns bunch spacing and 2.2×10^{11} ppb with 25 ns bunch spacing, respectively.

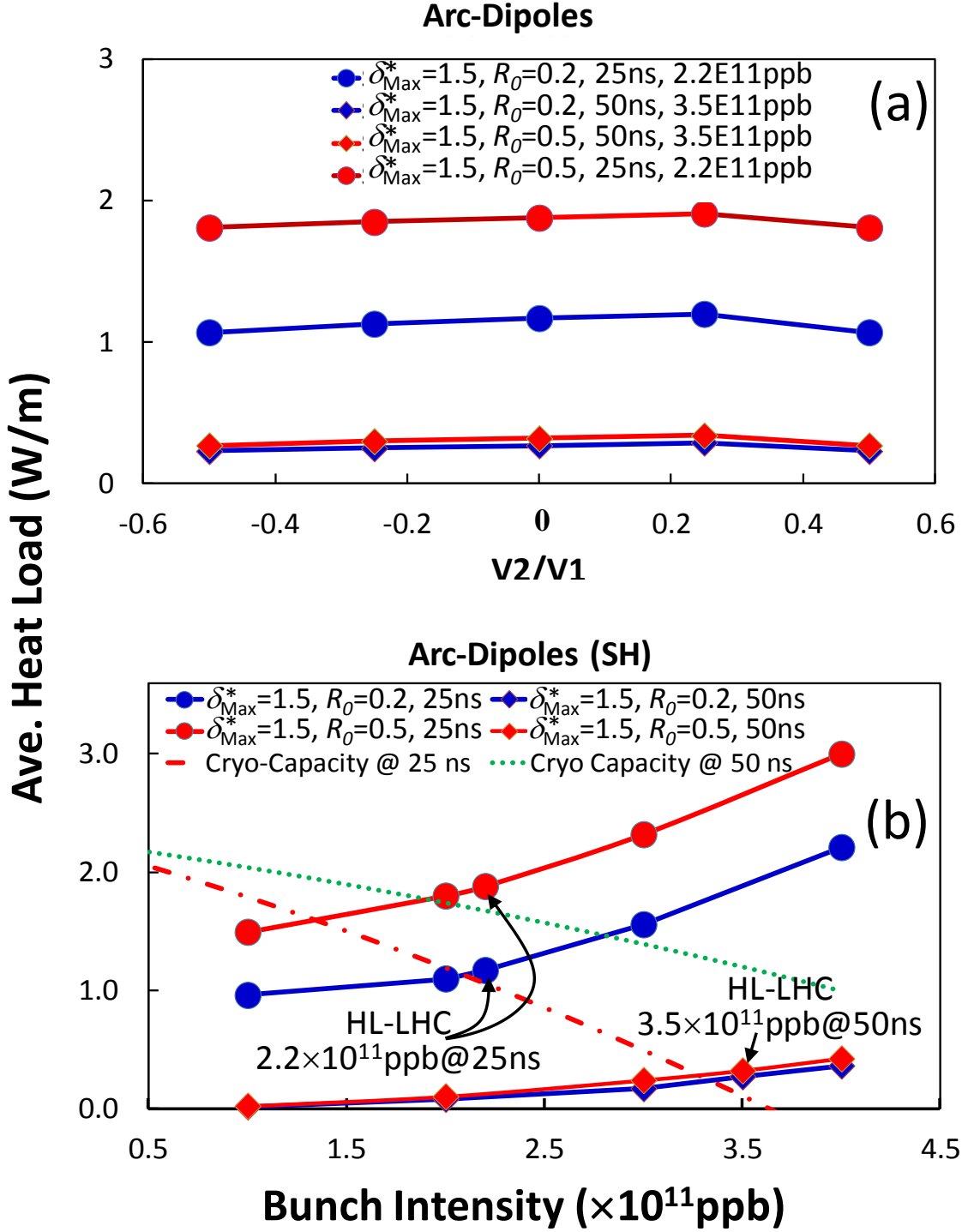


FIG. 13. Calculated average heat load for the HL-LHC beam scenarios: a) bunch profile dependence (left-most points are for BML50 and rightmost points are for BSM50, the points at $V2/V1 = 0$ are for the SH). b) Bunch intensity dependence. All of them use, photoelectron generation rate $[(e/p)/m]=0.00087$ [26].

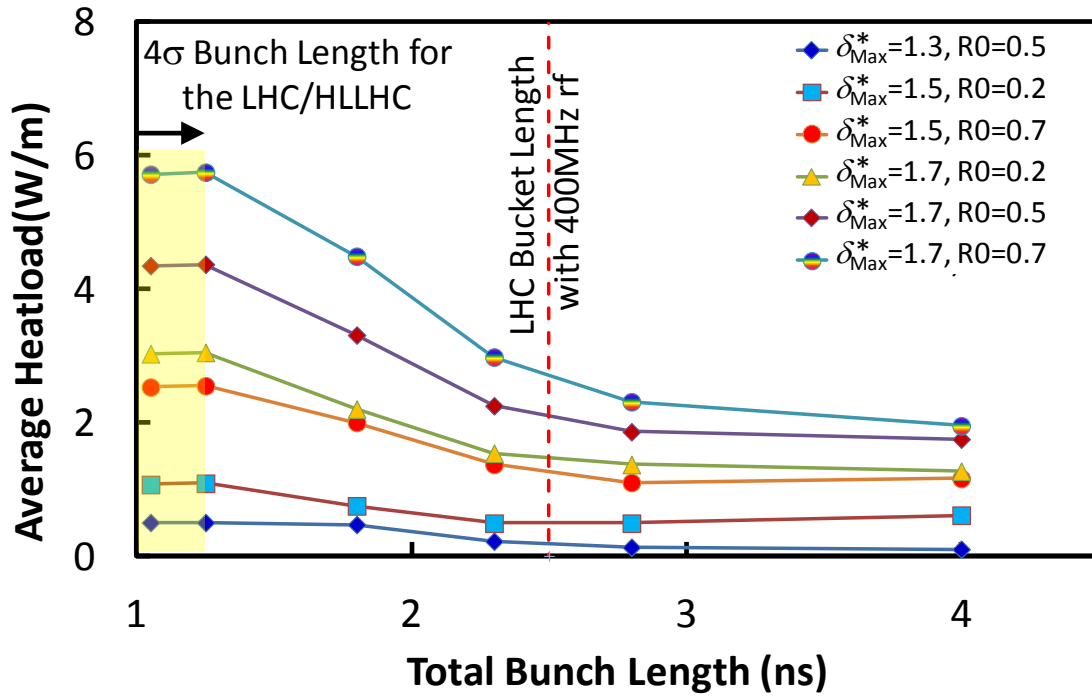


FIG. 14. Average heatload as a function of total bunch length for flat bunches in the LHC and for different values of secondary emission parameters. The assumed bunch population was 2.2×10^{11} ppb with 25 ns bunch spacing. The bucket length for the 400 MHz rf wave is shown by red dashed line. The shaded region indicates acceptable bunch lengths for the current LHC and the HL-LHC assuming 16 MV on the 400 MHz rf with beam emittance < 2.5 eVs.